

Biosorption Isotherms and Kinetics Studies for the Removal of 2,6-Dichlorophenolindophenol Using Palm Tree Trunk (*Elaeis guineensis*)

Marcel Cédric Deussi Ngaha, Lydiane Ghislaine Djemmoé, Evangéline Njanja*, Ignas Tonle Kenfack

Electrochemistry and Chemistry of Materials, Department of Chemistry, Faculty of Science, University of Dschang, Dschang, Cameroon
Email: *evangelinenjanja@yahoo.fr

How to cite this paper: Ngaha, M.C.D., Djemmoé, L.G., Njanja, E. and Kenfack, I.T. (2018) Biosorption Isotherms and Kinetics Studies for the Removal of 2,6-Dichlorophenolindophenol Using Palm Tree Trunk (*Elaeis guineensis*). *Journal of Encapsulation and Adsorption Sciences*, 8, 156-177.

<https://doi.org/10.4236/jeas.2018.83008>

Received: July 10, 2018

Accepted: September 9, 2018

Published: September 12, 2018

Copyright © 2018 by authors and Scientific Research Publishing Inc.

This work is licensed under the Creative Commons Attribution International License (CC BY 4.0).

<http://creativecommons.org/licenses/by/4.0/>



Open Access

Abstract

In this work, the potential of natural and pretreated palm tree trunk (PTT) as agents for adsorption of an organic dye, 2,6-dichlorophenolindophenol (2,6-DCPIP) from aqueous solutions was probed. Natural and acetic acid treated PTT were characterized by Fourier transform infrared (FT-IR) spectroscopy and by the point of zero charge (pzc). The biosorption of 2,6-DCPIP was investigated in batch mode using natural and treated PTT. This study was achieved by highlighting several parameters such as the contact time, biosorbents dosage, the initial concentration of 2,6-DCPIP, the pH of the solution, the ionic strength and the interfering ions. The results showed that 2,6-DCPIP was successfully adsorbed from aqueous solutions by natural and treated PTT. The equilibrium was attained after 40 minutes for treated PTT and 20 minutes for natural PTT. The maximum capacity of adsorption was obtained at pH = 2. The adsorption isotherms were investigated and it was found that the experimental data were best described by the Dubinin-Radushkevich isotherm for the natural PTT ($R^2 = 0.979$) and by the Temkin isotherm for the treated PTT ($R^2 = 0.976$). The maximum adsorption capacities determined by Langmuir isotherm were found as 108.932 and 157.233 $\mu\text{mol}\cdot\text{g}^{-1}$ for natural and treated PTT, respectively. The adsorption kinetics was analyzed and was best described by the pseudo-second order model ($R^2 \geq 0.998$). The diffusion mechanism was studied and the result showed that external mass transfer is the main rate controlling step. The desorption of 2,6-DCPIP is favorable in alkaline medium.

Keywords

Biosorption, Palm Tree Trunk, 2,6-Dichlorophenolindophenol, Isotherms, Kinetics, Desorption

1. Introduction

Dyes are synthetic aromatic water-soluble dispersible organic colorants, having potential applications in various industries. They are widely used in textile, paper, plastic, food and cosmetic industries in order to give the certain coloration to the desired product and also consume substantial volumes of water. It is reported that, over 100,000 dyes are commercially available and more than 700,000 ton/year are produced in the world [1] [2]. Most of the dyes are highly toxic, mutagenic, carcinogenic and recognized pollutants [3] [4] [5]. It is for this reason that, some dyes discharged from the effluents of these industries into receiving streams are sources of water pollution. Water effluents containing dyes have a very hazardous impact on environment, thus causing chronic and acute diseases [6]. Dyes can significantly affect visibility, photosynthesis and also aquatic life due to the presence of aromatics, metals and chlorides [7]. Hence the elimination of dyes from waste water is essential to prevent continuous environmental pollution. The commonly used procedures for removing organic dyes from aqueous solution include flocculation, electroflotation, chemical precipitation, electrokinetic coagulation, ion exchange, membrane filtration, electrochemical destruction, irradiation, ozonation and microbial biodegradation [1] [8] [9]. However, these methods are ineffective, non-economical and have many disadvantages such as high reagent and energy requirements, generation of toxic sludge or other waste products that require disposal or treatment [5]. There is thus a need to search for new processes that could remove organic dyes. The adsorption technique is one of the preferred methods of advanced wastewater treatment which industries employ to reduce hazardous organic dyes present in the effluent because it is efficient, simple to design and does not produce any sludge [1] [2] [10] [11]. At first, the adsorbent used in adsorption was commercial activated carbon. However, the high cost of activated carbon used in adsorption and problems of regeneration of adsorbent after adsorption [12] led to the search for new adsorbents that are lower in cost, locally available and efficient [11]. Several researchers were led to the use of agricultural solid wastes. Ever since, many agricultural solid wastes were used to adsorb organic dyes in aqueous solutions. Examples are: rice husk, tea leaves, orange peel, corncobs, coconut husk, barley husks, peanut hull, coir pith, wheat bran, eggshell, cocoa shell [2], hazelnut shells [13], olive stone [14], sugarcane bagasse [15] and wood sawdust [16]. All of these are excellent for organic dyes removal. The aim of this study was to investigate about a natural and abundant lignocellulosic material, palm tree trunk, for the adsorption of organic dyes which are mostly toxic nowadays. 2,6-DCPIP was chosen as an example of an organic dye. The effects of some important parameters such as treatment of biosorbent, initial dye concentration, pH of solution, adsorbent dosage, ionic strength, contact time and interfering ions on the adsorption of 2,6-DCPIP onto both natural and treated PTT were compared. The possibility to reuse the materials was also examined.

2. Materials and Methods

2.1. Materials, Preparation and Characterization of Biomass

All chemical reagents used in this experiment were of analytical grade, purchased and used without further purification. NaCl, CaCl₂ and NaOH were purchased from Fisher, CH₃COOH and BaCl₂ were purchased from BDH, HNO₃ and 2,6-DCPIP were purchased from Riedel-de-Häen and HCl was purchased from Phillip Harris. The structure of 2,6-DCPIP is illustrated in **Figure 1**.

The palm tree trunk used in this work was collected from a local agricultural field of the Littoral region in Cameroon. The biomass was cut into small pieces, washed several times with tap water to remove dust and soil particles, and then dried in sun for 8 days. The dried biomass was ground into fine powder and sieved to obtain sizes ranging from 0 - 100 μm. The powder was washed several times with distilled water, air-dried for 2 days and then in an oven at 110°C for 24 h before being kept in a bottle for further use.

In view of studying the effect of chemical pretreatment of biomass on 2,6-DCPIP uptake capacity, the biomass was submitted to pretreatment with acetic acid, according to the following procedure: 5 g of the natural biomass was put into contact with 100 mL of 2 mol·L⁻¹ acetic acid solution. The mixture was stirred in a mechanical platform shaker (EDMUND BÜHLER GmbH) for 2 h at a speed of 200 rpm. The resultant biomass was washed several times with distilled water in order to remove the excess of acetic acid until the pH (6.3) of washed water was stable. After washing thoroughly, the biosorbent was air-dried for 2 days and then in an oven at 110°C for 24 h before being kept in a bottle for further use.

The determination of the pzc of natural PTT and treated PTT was performed according to the method previously described by [17]. The pzc was measured by adding 0.1 g of biomass to 50 mL of 0.1 mol·L⁻¹ NaCl solution whose initial pH (pH_i) was measured and adjusted between 1 and 12 with NaOH or HCl solutions. The containers were sealed and placed on a mechanical platform shaker for 48 h at a speed of 150 rpm after which the final pH (pH_f) was measured. The pzc occurs when there is no change in pH after contact with the biosorbent. The pzc corresponds to the point where the curve of $\Delta\text{pH} = \text{pH}_f - \text{pH}_i = f(\text{pH}_i)$ crosses the line pH_i.

The natural and treated PTT were also characterized by using Fourier transform infrared spectroscopy (FT-IR) which allowed to identify different chemical

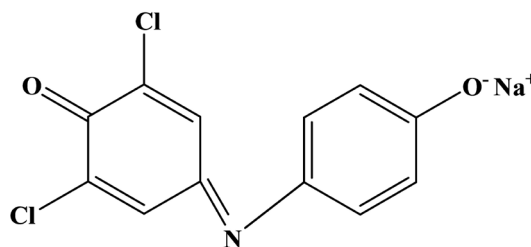


Figure 1. Chemical formula of 2,6-dichlorophenolindophenol [4].

functional groups present in natural and treated PTT powder. FT-IR spectra were obtained by means of the ATR technique with a Bruker α -P FT-IR spectrophotometer within a range of 4000 - 400 cm^{-1} with a resolution of 4 cm^{-1} ; 200 scans were collected for each spectrum.

2.2. Batch Biosorption and Desorption Studies

The stock solution of 2,6-DCPIP was prepared at 10^{-3} $\text{mol}\cdot\text{L}^{-1}$ by dissolving 0.327 g of the hydrated sodium salt of 2,6-dichlorophenolindophenol in 1 L of distilled water. Solutions of different concentrations (2×10^{-5} - 10^{-4} $\text{mol}\cdot\text{L}^{-1}$) were prepared by dilution of the stock solution with distilled water. The pH of each solution of 2,6-DCPIP was adjusted to the required value using HCl or NaOH solutions.

The biosorption studies were achieved in aqueous solution, in a shake flask, at room temperature. In this study, the batch biosorption experiments were carried out by mixing pre-weighted amounts (5 - 60 mg) of biosorbent with 10 mL of 2,6-DCPIP of various initial concentrations (2×10^{-5} - 10^{-4} $\text{mol}\cdot\text{L}^{-1}$) into a flask. The mixture was stirred at constant agitation speed of 150 rpm for an interval time between 5 - 70 min on a mechanical platform shaker. After agitation, the suspensions were filtered using whatman filter paper. The filtrates were analyzed by measuring the absorbance using UV-Vis Spectrophotometer (JENWAY) at a maximum adsorption wavelength of 600 nm [4]. The obtained absorbance was converted to the corresponding concentration C_e by using the equation of calibration curve. The amount of 2,6-DCPIP adsorbed at equilibrium q_e ($\text{mol}\cdot\text{g}^{-1}$) (Equation (1)), at time t q_t ($\text{mol}\cdot\text{g}^{-1}$) (Equation (2)) and the percentage of adsorption ($\%_{\text{ads}}$) (Equation (3)) were calculated as follows [14] [18] [19]:

$$q_e = \frac{C_i - C_e}{m} V_s \quad (1)$$

$$q_t = \frac{C_i - C_t}{m} V_s \quad (2)$$

$$\%_{\text{ads}} = \frac{C_i - C_e}{C_i} 100 \quad (3)$$

where C_i , C_e and C_t ($\text{mol}\cdot\text{L}^{-1}$) are the initial concentration, the final concentration at equilibrium and the final concentration at time t of 2,6-DCPIP, respectively. V_s (L) is the volume of 2,6-DCPIP solution and m (g) is the weight of the biosorbent.

The desorption studies were achieved by mixing 300 mg of biosorbents with 100 mL of 2,6-DCPIP of initial concentrations 10^{-4} $\text{mol}\cdot\text{L}^{-1}$ into a flask. The mixtures were stirred at constant agitation speed of 150 rpm for 40 min. After agitation, the suspensions were filtered using whatman filter paper. The filtrates were analyzed by measuring the absorbance using UV-Vis Spectrophotometer. The 2,6-DCPIP loaded biosorbents were recovered and dried in an oven. After drying, 30 mg of 2,6-DCPIP loaded biosorbents were mixed with 10 mL of the desorption solutions of H_2O , 10^{-2} $\text{mol}\cdot\text{L}^{-1}$ of NaOH or HNO_3 . The mixtures were

stirred at constant agitation speed of 150 rpm for 40 min on a mechanical platform shaker. After agitation, the suspensions were filtered. The filtrates were also analyzed by measuring the absorbance using UV-Vis Spectrophotometer. The desorption percentages ($\%_{\text{des}}$) were calculated as follows (Equation (4)) [20]:

$$\%_{\text{des}} = \frac{C_f - C_r}{C_f} 100 \quad (4)$$

where; C_f and C_r ($\text{mol}\cdot\text{L}^{-1}$) are the initial concentration and the final concentration of 2,6-DCPIP loaded biosorbents, respectively.

3. Results and Discussion

3.1. Characterization of Biomass

3.1.1. Fourier Transform Infrared (FT-IR) Spectroscopy

The FT-IR spectra of PTT were recorded in order to explore the surface functional groups as shown in **Figure 2(a)**. The spectra showed the presence of a broad peak, characteristic of OH group in the region $3400 - 3200 \text{ cm}^{-1}$, this peak shows the presence of alcohol, phenol or carboxylic acids [21] [22]. Another major peak detected at 2915.89 cm^{-1} was attributed to asymmetric and symmetric C - H stretching of aliphatic methyl and methylene. The peaks localized at 1725.38 cm^{-1} and 1628.20 cm^{-1} are characteristic of carbonyl (C = O) of carboxylic acids and carboxylate, respectively. The peak at 1510.65 cm^{-1} is a constant value for all the lignin esters. The IR peak at 1422.53 cm^{-1} may be due to the symmetrical bending vibration of alkane bonds ($-\text{CH}_2$). The absorption peak at 1238.72 cm^{-1} could be due to C - O, C - H or C - C stretching vibrations of carboxyl groups ($-\text{COOH}$). The band localized at 1031.92 cm^{-1} is attributed to C - O stretching vibrations of lignin [21] [22]. The region below 1000 cm^{-1} is the fingerprint zone and the absorption cannot clearly be assigned to any particular vibration because they correspond to complex interacting vibration systems [22]. The FT-IR spectrum of natural and treated PTT had similar bands with distinctive peak intensities (**Figure 2**).

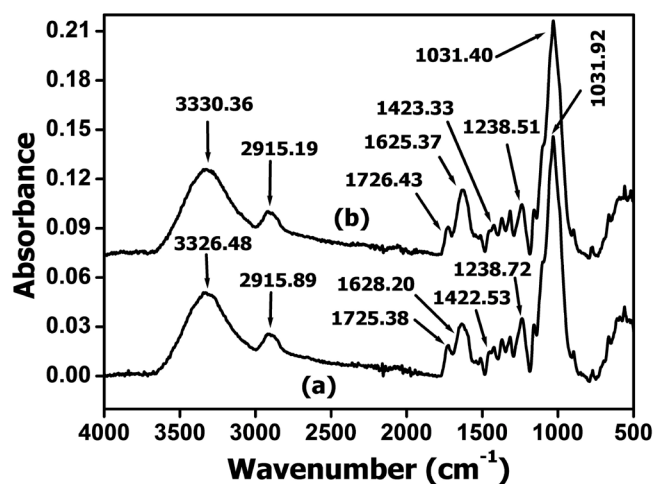


Figure 2. FT-IR spectra of (a) natural PTT and (b) treated PTT.

3.1.2. Point of Zero Charge (pzc)

The pzc of a material in a solution is the pH value at which the net surface charge of the material is equal to zero [17]. The **PZC** value of PTT was 4.8 (Figure 3), indicating that when the pH < 4.8, the surface of the material behaves as bases, fix protons contained in solution and become positively charged. This can be explained by the fact that the protons in solution migrate into PTT and settle on the carboxylate and hydroxyl function with which they interact to form a protonated material that is positively charge. This protonation increases the pH of the solution after equilibrium. On the other hand, when the pH > 4.8, the surface of material behaves as acids, releasing protons into the medium and become negatively charged. This can be explained by the dissociation of acidic functional groups of materials such as carboxylic acids involving the decreasing of the pH of the solution after equilibrium [17] [23].

The pzc value of the pretreated PTT with acetic acid (3.8) is lower than the pzc value of PTT (Figure 3). This decrease in pzc values can be explained by the fact that the treatment with acetic acid involves the reduction of basic functions and an increase in acidic functions that result to the action of this acid on the biosorbent.

3.2. Effect of Pretreatment of Biomass

The biosorbent was treated with acetic acid. The treatment affected the functional groups contained at the surface of the material. Figure 4 shows the effect of chemical treatment on the biosorption of 2,6-DCPIP. It can be observed from this figure that the amount of 2,6-DCPIP adsorbed at equilibrium is 20.303 $\mu\text{mol}\cdot\text{g}^{-1}$ for natural PTT and 26.007 $\mu\text{mol}\cdot\text{g}^{-1}$ for treated PTT. As can be seen, the amount of 2,6-DCPIP adsorbed at equilibrium is higher with treated PTT than natural PTT. This result can be explained by the fact that the treatment with acetic acid like all the acid treatments, lead to the protonation of the surface functional groups of the material [22], which increased the electrostatic interaction between the positively charged surface of the material and the negatively charged molecules of 2,6-DCPIP.

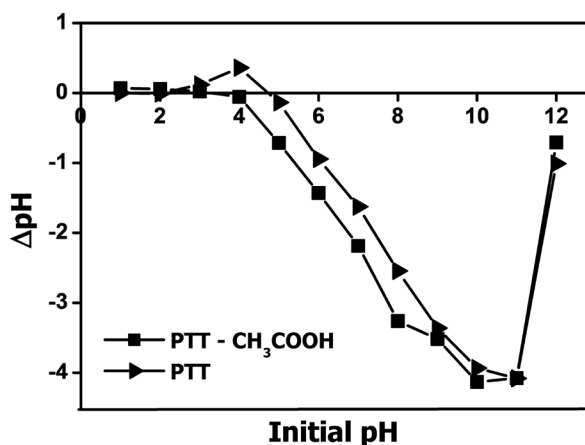


Figure 3. Graph of point of zero charge.

3.3. Effect of Biosorbents Dosage

The effect of biosorbents dosage on the removal of 2,6-DCPIP was studied and the results of this study are shown in **Figure 5**. The removal percentage of 2,6-DCPIP increased from 8.251% to 81.169% and from 22.789% to 89.755% for natural and treated PTT, respectively. As can be seen, the removal percentage of 2,6-DCPIP increased considerably with increasing adsorbent dosage. This is because of the greater surface area, the availability of more adsorption sites (carboxyl groups) for 2,6-DCPIP adsorption during the adsorption reaction [19]. A further increase in adsorbent dosage for treated PTT (>4.0 g/L) did not cause significant improvement in 2,6-DCPIP adsorption. This may be due to the adsorption of almost all the 2,6-DCPIP onto the biosorbent and the establishment of equilibrium. This situation can also be attributed to overlapping of adsorption sites as a result of overcrowding of biomass [24]. A quite similar tendency was reported by [19] for the adsorption of malachite green by sea shell powder.

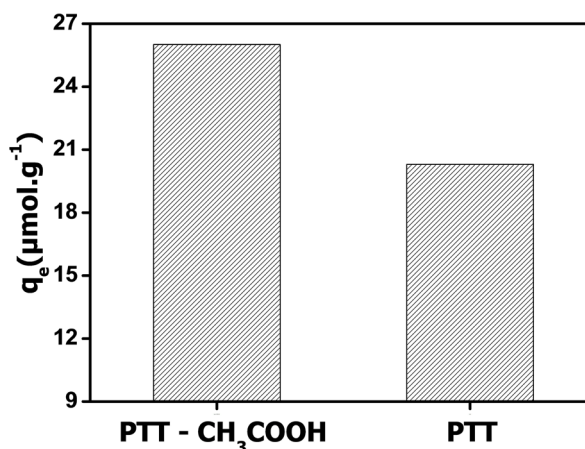


Figure 4. Effect of pretreatment of PTT on the biosorption of 2,6-DCPIP. Experimental conditions: [2,6-DCPIP] = 10^{-4} mol·L⁻¹; m = 3 g·L⁻¹; G = 0 - 100 μm ; t = 40 min; v = 150 rpm; V = 10 mL; pH = 6.7; at room temperature.

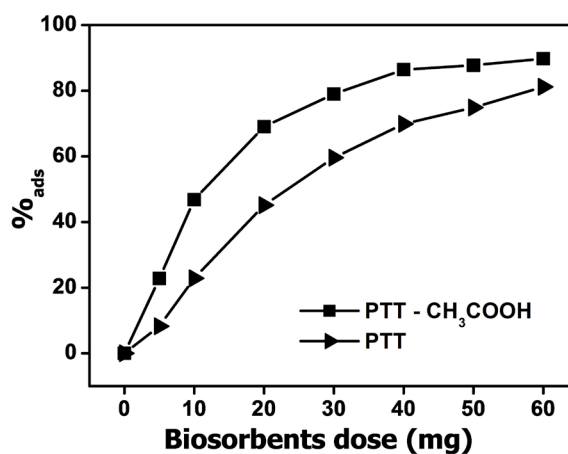


Figure 5. Effect of biosorbents dose on the biosorption of 2,6-DCPIP. Experimental conditions: [2,6-DCPIP] = 10^{-4} mol·L⁻¹; G = 0 - 100 μm ; t = 40 min; v = 150 rpm; V = 10 mL; pH = 6.7; at room temperature.

3.4. Effect of Contact Time

The effect of contact time on biosorption of 2,6-DCPIP is presented in **Figure 6**. It can be observed from this figure that, rapid adsorption of 2,6-DCPIP takes place in the first 5 minutes for the two materials, thereafter, the rate of adsorption decreases gradually with the progress of adsorption and reaches equilibrium in about 20 minutes for natural PTT and 40 minutes for treated PTT. No significant change in 2,6-DCPIP removal is obtained after the equilibrium time. The initial rapid phase may be due to rapid attachment of 2,6-DCPIP to the biosorbent surface or to the availability of more adsorption vacant sites at the initial stage [15]. But after some of the easily available active sites are used up, the dye needs some time to find out more active sites for binding until the equilibrium time is reached [10] [25].

3.5. Effect of Initial Concentration

The effect of initial concentration on the biosorption of 2,6-DCPIP was investigated and the results are shown in **Figure 7**. It can be observed from this figure that, the amount of 2,6-DCPIP adsorbed at equilibrium increases from 3.690 to 18.395 $\mu\text{mol}\cdot\text{g}^{-1}$ and from 4.644 to 23.451 $\mu\text{mol}\cdot\text{g}^{-1}$ for natural and treated PTT, respectively. As can be seen, the amount adsorbed at equilibrium for both biosorbents increases as the 2,6-DCPIP concentration increases. This result can be explained by the fact that increasing the initial 2,6-DCPIP concentration would increase the mass transfer driving force, and hence, the rate at which 2,6-DCPIP molecules pass from solution to the particle surface [8] [3] [19]. This behaviour suggests that available sites on the biosorbent are the limiting factor for the 2,6-DCPIP removal [15].

3.6. Effect of Solution pH

The pH is an important factor that affects biosorption processes. It is used in

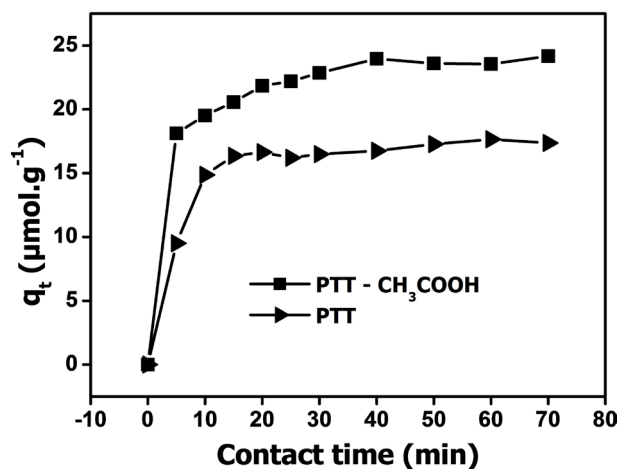


Figure 6. Effect of contact time on the biosorption of 2,6-DCPIP. Experimental conditions: [2,6-DCPIP] = 10^{-4} mol·L⁻¹; m = 3 g·L⁻¹; G = 0 - 100 μm ; v = 150 rpm; V = 10 mL; pH = 6.7; at room temperature.

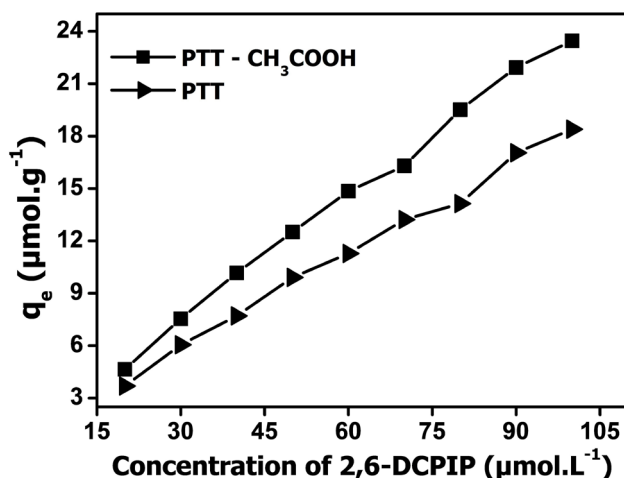


Figure 7. Effect of initial concentration on the biosorption of 2,6-DCPIP. Experimental conditions: $m = 3 \text{ g.L}^{-1}$; $G = 0 - 100 \mu\text{m}$; $t = 40 \text{ min}$; $v = 150 \text{ rpm}$; $V = 10 \text{ mL}$; $\text{pH} = 6.7$; at room temperature.

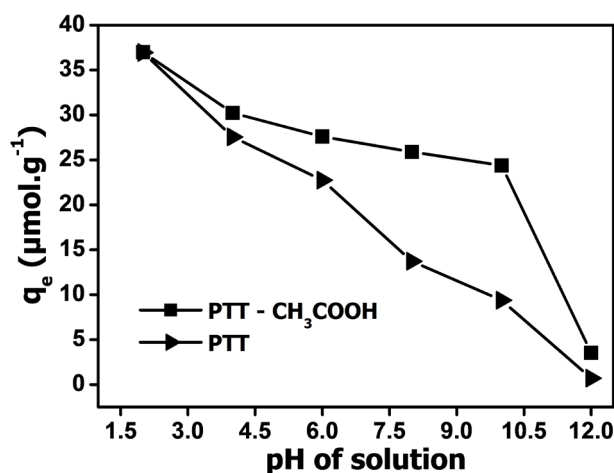


Figure 8. Effect of pH of solution on the biosorption of 2,6-DCPIP. Experimental conditions: $[\text{2,6-DCPIP}] = 10^{-4} \text{ mol.L}^{-1}$; $m = 3 \text{ g.L}^{-1}$; $G = 0 - 100 \mu\text{m}$; $t = 40 \text{ min}$; $v = 150 \text{ rpm}$; $V = 10 \text{ mL}$; at room temperature.

industry to increase the adsorption of dyes. The effect of initial pH on biosorption of 2,6-DCPIP on natural and treated PTT is shown in **Figure 8** and the results indicate that, the maximum capacity of adsorption is obtained at $\text{pH} = 2$. When the pH increases, the capacity of adsorption decreases from 36.955 to $0.706 \mu\text{mol.g}^{-1}$ and from 36.993 to $3.529 \mu\text{mol.g}^{-1}$ for natural and treated PTT, respectively. This can be explained by the fact that, the **PZC** of natural PTT is 4.8 and treated PTT is 3.8 . Thus, at low pH ($\text{pH} < \text{PZC}$) more protons will be available for the protonation of the biosorbent surface which increases the electrostatic attraction between the positively charged biosorbent sites and the negatively charged 2,6-DCPIP. There is nearly no electrostatic repulsion between the biosorbent and the 2,6-DCPIP at $\text{pH} = 2$ and hence, the amount adsorbed is at its maximum. Increasing the pH ($\text{pH} > \text{PZC}$) leads to an increase in 2,6-DCPIP anions in the solution as well as the number of negatively charged sites on the

adsorbent due to the increase in hydroxyl ions. This results in electrostatic repulsion between the 2,6-DCPIP and the adsorbent, which is the reason for the decrease in the amount of adsorption. A similar trend was observed for the adsorption of azo dyes by glutaraldehyde-crosslinked chitosans [26].

3.7. Effect of Ionic Strength

The ionic strength of the solution is one of the factors that control both electrostatic and non-electrostatic interactions between the adsorbate and the adsorbent surface [7]. The effect of ionic strength on biosorption of 2,6-DCPIP was carried out using the initial concentration of NaCl. The results illustrated in **Figure 9** reveal that an increase of ionic strength causes an increase in the adsorption capacity of the 2,6-DCPIP. This result can be explained by the fact that the addition of salt increases the aggregation of dye molecules and decreases the solubility. An increase in aggregation promotes the adsorption of dye molecules [7] [27]. Another possibility is that an increase in ionic strength increases the positive charge of the biosorbent surface, thus increasing the electrostatic attraction between dye (2,6-DCPIP) and biosorbent [28]. Additionally, an increase in ionic strength of aqueous solution may result in the compression of the diffuse double layer on the biosorbent. This eases the electrostatic attraction and consequently participates in adsorption [8].

3.8. Effect of Interfering Ions

The effect of interfering ions on biosorption of 2,6-DCPIP was carried out using different salts; BaCl₂, CaCl₂ and NaCl. The results show that the capacity of adsorption increases with the presence of salts in the order NaCl < CaCl₂ < BaCl₂ (**Figure 10**). The capacity of adsorption is higher with divalent ions. This is because the doubly charged ions increase the surface charges of biosorbents, which increases the electrostatic interaction and/or anionic exchange between the

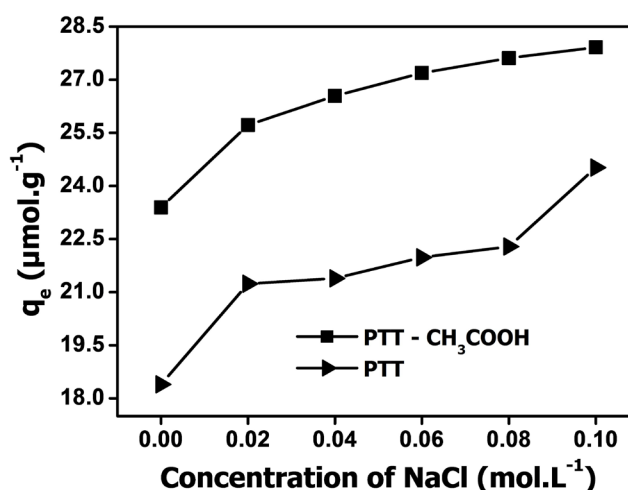


Figure 9. Effect of ionic strength on the biosorption of 2,6-DCPIP. Experimental conditions: [2,6-DCPIP] = 10⁻⁴ mol.L⁻¹; m = 3 g.L⁻¹; G = 0 - 100 μm; t = 40 min; v = 150 rpm; V = 10 mL; pH = 6.7; at room temperature.

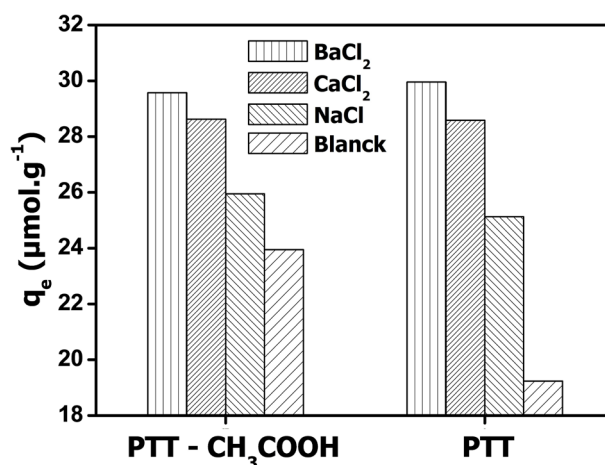


Figure 10. Effect of interfering ions on the biosorption of 2,6-DCPIP. Experimental conditions: [2,6-DCPIP] = 10^{-4} mol·L⁻¹; $m = 3$ g·L⁻¹; $G = 0 - 100$ μm; $t = 40$ min; $v = 150$ rpm; $V = 10$ mL; $pH = 6.7$; at room temperature.

2,6-DCPIP and the biosorbents. This can also be explained by the fact that the divalent ions favour more aggregation of dye molecules and decreases the solubility than the monovalent ions. The higher capacity of adsorption of BaCl₂ than CaCl₂ can be explained by the fact that, the higher molecular weight of BaCl₂ favours more aggregation of dye molecules and decreases the solubility than the lower molecular weight of CaCl₂.

3.9. Adsorption Isotherms

In order to understand the mechanism of biosorption, it is important to perform the adsorption isotherms. In this study, four adsorption isotherms were used to describe the obtained equilibrium data: Langmuir, Freundlich, Dubinin-Radushkevich and Temkin isotherms.

3.9.1. Langmuir Isotherm

The general equation of Langmuir isotherm is described as follows (Equation (5)) [12] [29]:

$$\frac{C_e}{q_e} = \frac{1}{K_L \cdot q_{\max}} + \frac{C_e}{q_{\max}} \quad (5)$$

where; q_e and q_{\max} (μmol·g⁻¹) are the equilibrium and maximum biosorption capacities of biosorbent, respectively. C_e (μmol·L⁻¹) is the equilibrium concentration of solution. K_L (L·μmol⁻¹) is the Langmuir biosorption constant. The constants q_{\max} and K_L were calculated from the slopes and intercepts of linear plots of $\frac{C_e}{q_e}$ versus C_e . The essential characteristic of Langmuir isotherm

can be expressed in terms of a dimensionless constant called separation factor (R_L), which is defined as follows (Equation (6)) [30]:

$$R_L = \frac{1}{1 + K_L C_i} \quad (6)$$

The value of R_L indicates whether the type of adsorption isotherm will be favorable ($R_L < 1$), unfavorable ($R_L > 1$), linear ($R_L = 1$) or irreversible ($R_L = 0$).

3.9.2. Freundlich Isotherm

The general equation of Freundlich isotherm is described as follows (Equation (7)) [12] [29]:

$$\log q_e = \log K_f + \frac{1}{n} \log C_e \quad (7)$$

where K_f ($L \cdot g^{-1}$) is the Freundlich constant related to the biosorption capacity and $\frac{1}{n}$ is an empirical parameter related to the biosorption intensity of the adsorbent. The Freundlich isotherm constants $\frac{1}{n}$ and K_f were calculated from the slopes and intercepts of linear plots of $\log q_e$ versus $\log C_e$.

3.9.3. Dubinin-Radushkevich Isotherm

The general formula of Dubinin-Radushkevich isotherm is given by the following Equation (8) [14] [31]:

$$\ln q_e = \ln q_{\max} - \beta \varepsilon^2 \quad (8)$$

where; β ($\text{mol}^2 \cdot \text{kJ}^{-2}$) is the activity coefficient related to the mean free energy (E ($\text{kJ} \cdot \text{mol}^{-1}$)) obtained from Equation (10) and ε is polanyi potential which is determined from Equation (9):

$$\varepsilon = RT \ln \left(1 + \frac{1}{C_e} \right) \quad (9)$$

where, R is the universal gas constant ($8.314 \times 10^{-3} \text{ kJ} \cdot \text{mol}^{-1} \cdot \text{K}^{-1}$) and T is the absolute temperature in kelvin in our case (298 K). The constants β and q_{\max} were calculated from the slopes and the intercepts of linear plot of $\ln q_e$ versus ε^2 .

$$E = \frac{1}{\sqrt{-2\beta}} \quad (10)$$

3.9.4. Temkin Isotherm

The general formula of Temkin isotherm is given by the following Equation (11) [29] [31] [32]:

$$q_e = q_{\max} \frac{RT}{\Delta Q} \ln K_T + q_{\max} \frac{RT}{\Delta Q} \ln C_e \quad (11)$$

where; ΔQ ($\text{kJ} \cdot \text{mol}^{-1}$) is the heat of adsorption, K_T ($L \cdot \mu\text{mol}^{-1}$) is the Temkin isotherm constant. The constants ΔQ and K_T were calculated from the slopes and the intercepts of linear plot of q_e versus $\ln C_e$.

The isotherms obtained for 2,6-DCPIP adsorption onto natural and treated PTT are shown in **Figure 11** and the corresponding adsorption constants are

summarized in **Table 1**.

The values of correlation coefficients of Dubinin-Radushkevich and Temkin isotherms are closest to unity, implying that Dubinin-Radushkevich and Temkin isotherms are most appropriate to describe the biosorption of 2,6-DCPIP on natural and treated PTT, respectively. The values of $1/n$ determined by the Freundlich isotherm (**Table 1**) are less than unity, implying that biosorption is favorable for both biosorbents [12] [29] [32].

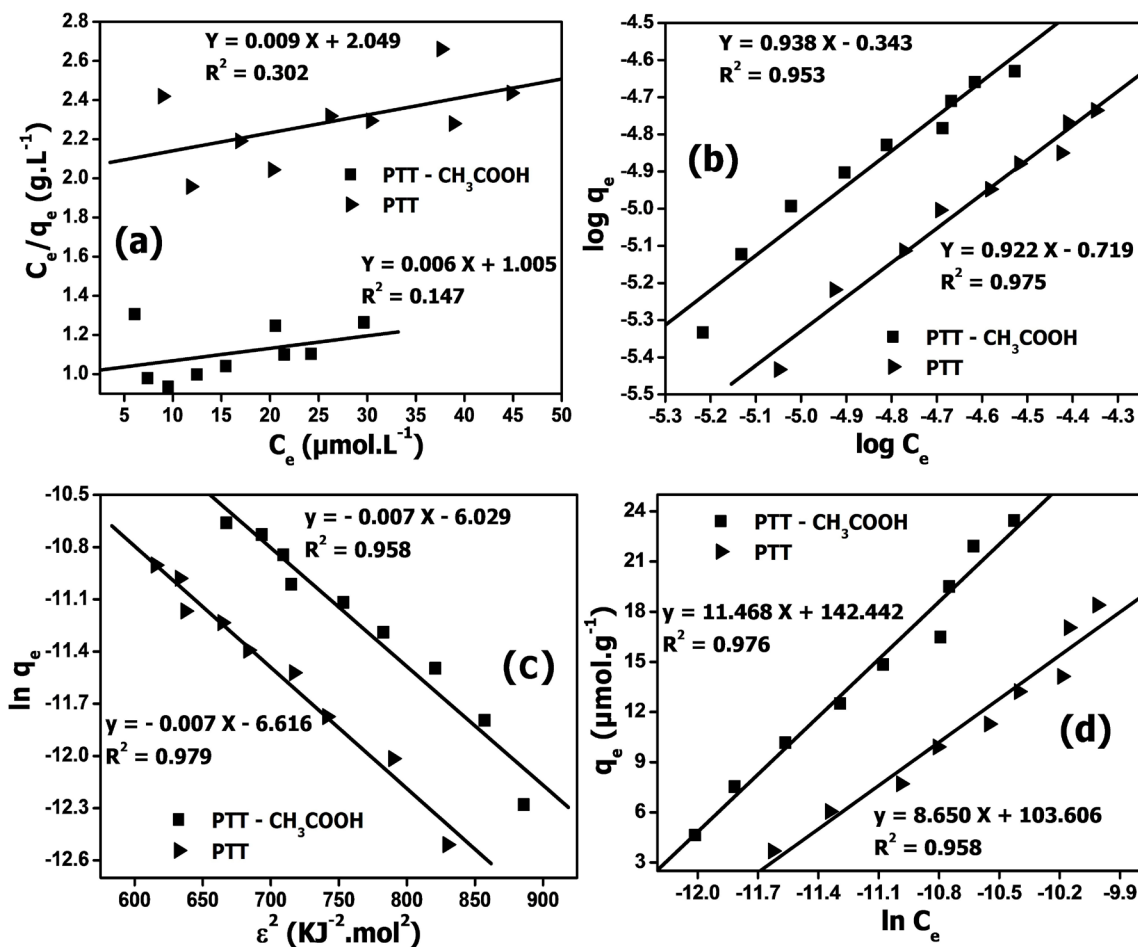


Figure 11. Adsorption isotherms of Langmuir (a), Freundlich (b), Dubinin-Radushkevich (c) and Temkin (d).

Table 1. Langmuir, Freundlich, Dubinin-Radushkevich and Temkin constants of adsorption.

Biosorbents	Langmuir			Freundlich		
	K_L (L.μmol ⁻¹)	q_{max} (μmol.g ⁻¹)	R^2	K_f (L.g ⁻¹)	$1/n$	R^2
PTT-CH ₃ COOH	0.006	157.233	0.147	0.454	0.938	0.953
PTT	0.004	108.932	0.302	0.191	0.922	0.975
Biosorbents	Dubinin-Radushkevich			Temkin		
	E (kJ.mol ⁻¹)	q_{max} (μmol.g ⁻¹)	R^2	ΔQ (kJ.mol ⁻¹)	K_T (L.μmol ⁻¹)	R^2
PTT-CH ₃ COOH	8.562	2409.033	0.958	33.969	0.248	0.976
PTT	8.476	1339.244	0.979	31.202	0.159	0.958

The adsorption energies obtained from Dubinin-Radushkevich isotherm (**Table 1**) are between 8 and 16 kJ·mol⁻¹, implying that chemisorption (anionic exchange) is the mechanism which controls the biosorption process [31]. The positive values of the heat of adsorption from Temkin isotherm (**Table 1**) indicate that the adsorption process is exothermic [28] [32]. Moreover, the heat of adsorption of treated PTT is greater than the heat of adsorption of natural PTT. This implies that interactions between 2,6-DCPIP ions and treated PTT are more energetic than interactions between 2,6-DCPIP ions and natural PTT [32].

The values of the separation factor determined by the Langmuir isotherm (**Figure 12**) are found between 0 - 1 (0.612 - 0.888 for treated PTT and 0.691 - 0.918 for natural PTT), meaning that biosorption is favorable for both biosorbents. This result is in agreement with what was already noted with the Freundlich isotherm. The lower R_L values at higher initial 2,6-DCPIP concentrations showed that the adsorption was more favorable at higher concentrations [33]. The values of R_L of treated PTT are lower than the values of natural PTT, implying that the adsorption of 2,6-DCPIP is more favorable with treated PTT rather than natural PTT [30].

3.10. Adsorption Kinetics

The controlling mechanisms of adsorption process such as chemical reaction, diffusion control or mass transfer coefficient are used to determine kinetic models. Thus, the kinetics of dye onto various adsorbent materials was analyzed using different kinetic models which are presented below.

3.10.1. Pseudo-First Order Model

The pseudo-first order equation of Lagergren is generally expressed as follows (Equation (12)) [14] [25] [34]:

$$\log(q_e - q_t) = \log q_e - \frac{K_1 \text{ads}}{2.303} t \quad (12)$$

where; q_e and q_t ($\mu\text{mol}\cdot\text{g}^{-1}$) are the amounts of 2,6-DCPIP adsorbed at

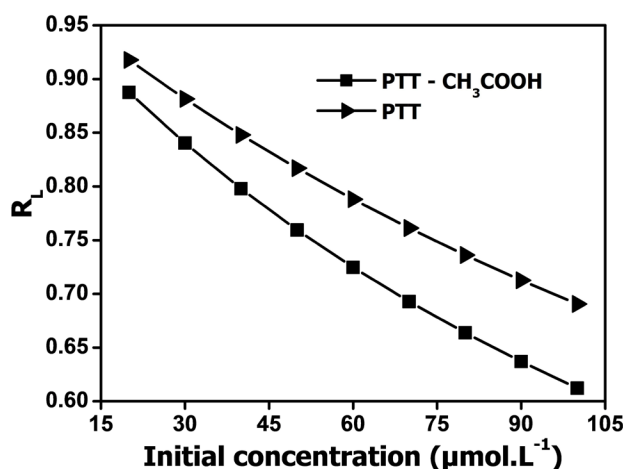


Figure 12. Evolution of separation factor against the initial concentration of 2,6-DCPIP.

equilibrium and at time t , respectively. $K_{1\text{ads}}$ (min^{-1}) is the rate constant of pseudo-first order. The values of $K_{1\text{ads}}$ and q_e were calculated from the slopes and intercepts of the linear plots of $\log(q_e - q_t)$ versus t .

3.10.2. Pseudo-Second Order Model

The pseudo-second order equation is generally expressed as follows (Equation (13)) [14] [25] [34]:

$$\frac{t}{q_t} = \frac{1}{K_{2\text{ads}} \cdot q_e^2} + \frac{1}{q_e} \cdot t \quad (13)$$

where $K_{2\text{ads}}$ ($\text{g} \cdot \mu\text{mol}^{-1} \cdot \text{min}^{-1}$) is the rate constant of pseudo-second order. The values of q_e and $K_{2\text{ads}}$ were calculated from the slopes and intercepts of the linear plots of $\frac{t}{q_t}$ versus t . This model allows determining the initial rate of reaction h ($\mu\text{mol} \cdot \text{g}^{-1} \cdot \text{min}^{-1}$) (Equation (14)) and the half time of the reaction $t_{1/2}$ (min) (Equation (15)).

$$h = K_{2\text{ads}} \cdot q_e^2 \quad (14)$$

$$t_{1/2} = \frac{1}{q_e \cdot K_{2\text{ads}}} \quad (15)$$

3.10.3. Elovich Model

The Elovich model is represented by the following Equation (16) [34]:

$$q_t = \frac{1}{\beta} \ln(\alpha\beta) + \frac{1}{\beta} \ln t \quad (16)$$

where; α ($\text{mmol} \cdot \text{g}^{-1} \cdot \text{min}^{-1}$) is the initial adsorption rate and β ($\text{g} \cdot \mu\text{mol}^{-1}$) is related to the extent of surface coverage and activation energy for chemisorption. The values of β and α were calculated from the slopes and intercepts of the linear plots of q_t versus $\ln t$.

3.10.4. Intraparticle Diffusion Model

Weber and Morris demonstrated that in intraparticle diffusion studies, rate processes are usually expressed in terms of square root of time [12] [19] [34]. The intraparticle diffusion model is defined by Equation (17).

$$q_t = K_{ip} t^{1/2} + C \quad (17)$$

where; K_{ip} ($\mu\text{mol} \cdot \text{g}^{-1} \cdot \text{min}^{-1/2}$) is the intraparticle diffusion rate constant and C ($\mu\text{mol} \cdot \text{g}^{-1}$) is the thickness of boundary layer. The values of K_{ip} and C were calculated from the slopes and intercepts of the linear plots of q_t versus $t^{1/2}$.

3.10.5. External Mass Transfer Resistance Model

This model assumes that the surface solute concentration C_s , on the sorbent is negligible at $t = 0$, and that intraparticle diffusion is also negligible; it is used to calculate the initial rate of solute sorption. The initial rate of sorption can be determined using the classical mass transfer equation, which describes the evolu-

tion of solute concentration C_t in solution (Equation (18)) [12] [35]:

$$\frac{dC_t}{dt} = -\beta_L S (C_t - C_s) \quad (18)$$

where; β_L is the external mass transfer coefficient, C_t is the liquid phase solute concentration at time t , C_s is the liquid phase solute concentration at the particle surface and S is the specific surface area for mass transfer. This equation can be simplified by substituting the following boundary conditions: $C_t \rightarrow C_0$ and $C_s \rightarrow 0$ when $t \rightarrow 0$; C_0 = initial solute concentration, to Equation (19) [12] [35]:

$$\frac{d(C_t/C_0)}{dt} = -\beta_L S \quad (19)$$

So the external mass transfer rate $\beta_L S$, was approximated by the initial slope of the C_t/C_0 versus time graph.

3.10.6. Boyd Model

In order to interpret the rate-controlling step during the adsorption process, the experimental data were further analyzed by the model given by Boyd (Equation (20)) [12] [29] [35]:

$$F = 1 - \frac{6}{\pi^2} \exp(-Bt) \quad (20)$$

Since $F = \frac{q_t}{q_e}$, Bt could be represented as follows (Equation (21)):

$$Bt = -0.4977 - \ln(1 - F) \quad (21)$$

where; F is the fraction of solute sorbed at different times t and Bt is a mathematical function of F . The calculated B values are used to calculate the effective diffusion coefficient, D_i (cm^2/s) using Equation (22) [35] [36]:

$$B = \frac{\pi^2 D_i}{r^2} \quad (22)$$

where, r represents the mean radius of the particle calculated by sieve analysis and by assuming them as spherical particles.

Kinetics of The 2,6-DCPIP adsorption onto natural and treated PTT are shown in **Figure 13** and the corresponding constants are given in **Table 2**.

Table 2 indicate that the pseudo-second order model adequately describes the adsorption kinetics of 2,6-DCPIP on the biosorbents with a high correlation coefficient. Moreover, it can be observed that the values of the calculated q_e of pseudo-second order model are in good agreement with experimental q_e values. This means that the biosorption of 2,6-DCPIP on biosorbents is a process that is controlled by chemisorption [10] [24] [25]. On the other hand, the low reaction half time and the high initial rate of reaction (**Table 2**) of treated PTT compared to natural PTT confirm that the biosorption of 2,6-DCPIP is very fast with treated PTT than natural PTT [17] [32].

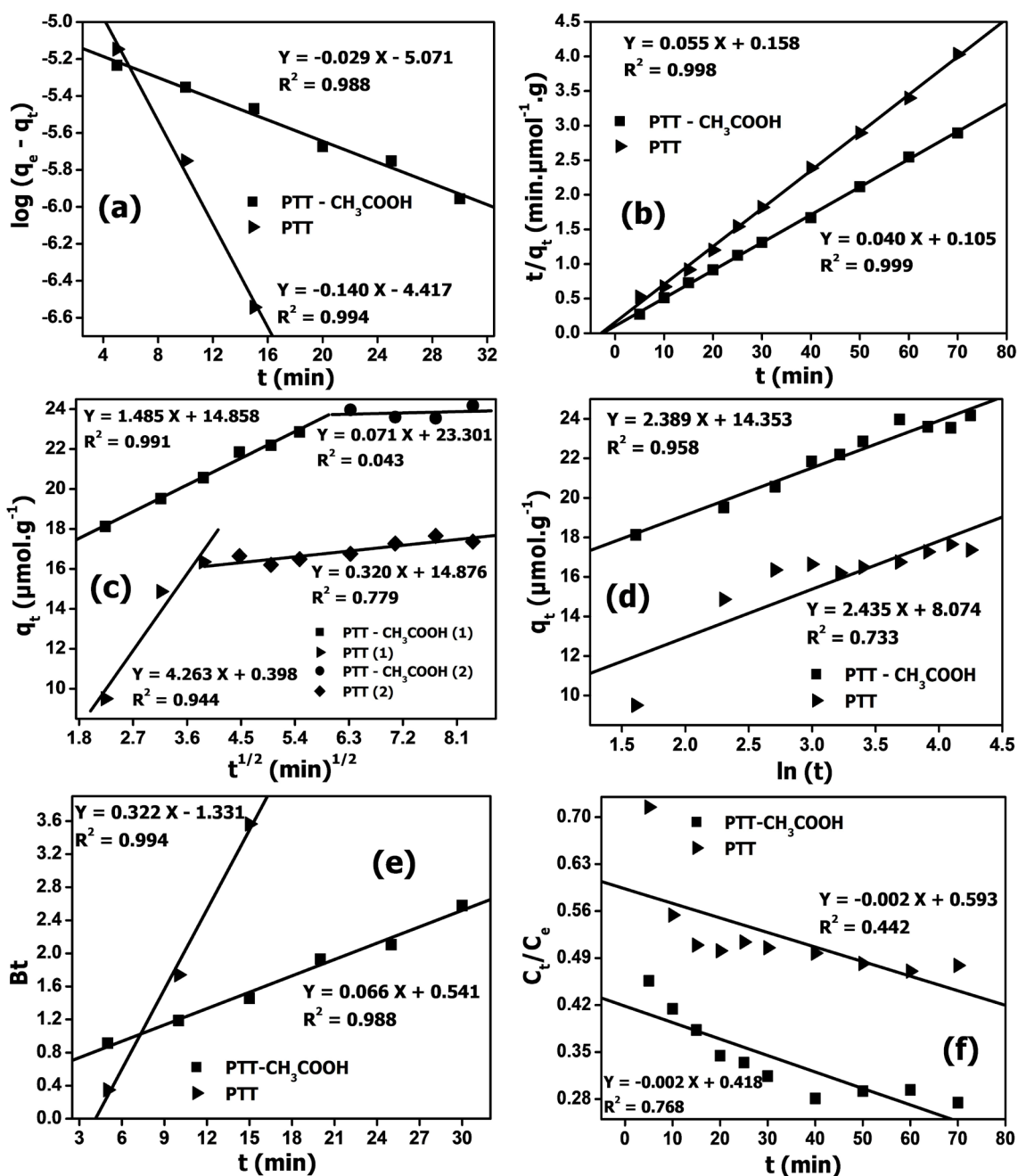


Figure 13. Kinetic adsorptions of pseudo-first order (a), pseudo-second order (b), intraparticle diffusion (c), Elovich (d), Boyd (e) and external mass transfer (f).

From **Figure 13(c)**, the curves of intraparticle diffusion present two linear portions. The first portion located at the beginning of the process is attributed to the film diffusion, where the 2,6-DCPIP diffuses through the solution to the external surface of adsorbent or boundary layer diffusion. The second portion located at the end of the process describes the pore diffusion [37]. It is also clear from **Figure 13(c)** and **Table 2** that the first stage is faster than the second one, which may be ascribed to the very slow diffusion of the 2,6-DCPIP from the surface film into the micropores which represent the least accessible sites for

Table 2. Pseudo-first order, Pseudo-second order, Elovich, Intraparticle diffusion, External mass transfer and Boyd constants of adsorption.

Biosorbents	Pseudo-first order model				Pseudo-second order model				
	q_{exp}	q_e	$k_{1,ms}$	R^2	q_e	$k_{2,ms}$	h	$t_{1/2}$	R^2
PTT-CH ₃ COOH	23.966	8.485	0.066	0.988	24.900	0.015	9.523	2.615	0.999
PTT	16.754	38.295	0.322	0.994	18.242	0.019	6.342	2.876	0.998
Biosorbents	Elovich model			External mass transfer		Boyd model			
	α	β	R^2	$\beta_i S \times 10^3$	R^2	B	$D_i \times 10^9$	R^2	
PTT-CH ₃ COOH	0.972	0.419	0.958	2.450	0.768	0.066	2.787	0.988	
PTT	0.067	0.411	0.733	2.170	0.442	0.322	13.592	0.994	
Biosorbents	Intraparticle diffusion model								
	k_{ip_1}	k_{ip_2}	C_1	C_2	R_1^2	R_2^2			
PTT-CH ₃ COOH	1.485	0.071	14.858	23.301	0.991	0.043			
PTT	4.263	0.320	0.398	14.876	0.944	0.779			

adsorption. Also, the intraparticle diffusion model curve does not pass through the origin, which is an indication that 2,6-DCPIP diffusion in the bulk of natural and treated PTT is not the only process that governs the biosorption [9] [15]. Moreover, the values of the thickness of boundary layer C for each linear portion are not zero, indicating that intraparticle diffusion is present as a part of diffusion process, but it is not the sole rate-controlling step in all the stages [29].

Figure 13(e) shows that the straight line obtained by the Boyd model does not pass through the origin of the graph, implying that external mass transfer is the main rate controlling step at the initial stages [12] [36]. The values of D_i presented in **Table 2** lie in the range 10^{-13} to 10^{-5} cm²/s, indicating that chemisorption occurs during the biosorption process [17]. This result is in agreement with the pseudo-second order model and Dubinin-Radushkevich isotherm. Thus, the biosorption of 2,6-DCPIP on the natural and treated PTT is best described by external mass transfer diffusion rather than internal diffusion.

3.11. Desorption

The repeated availability of the adsorbents after adsorption-desorption cycles is crucial to illustrate the stability and potential recovery of the adsorbents. In this study, NaOH, HNO₃ and H₂O were used as desorbing agents to regenerate the biosorbents. The results show that the maximum desorption percentage, 67.371% for natural PTT and 54.260% for treated PTT is obtained in NaOH medium (**Figure 14**). This can be explained by the phenomenon of anionic exchange between the hydroxyl ions (OH⁻) of NaOH solution and 2,6-DCPIP loaded biosorbent. However, the low percentage of desorption obtained with treated PTT compared to natural PTT is due to the strong bond formed between the 2,6-DCPIP and the treated PTT [20].

4. Conclusions

From this study, the capacity of using natural and treated PTT for the removal of

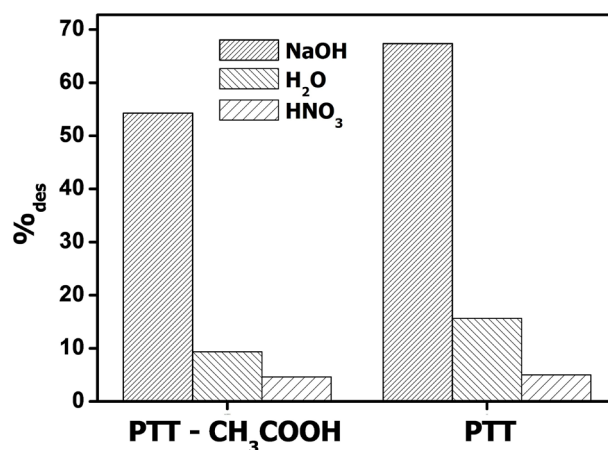


Figure 14. Effect of desorption solution on the recovery of adsorbed 2,6-DCPIP. Experimental conditions: 30 mg of 2,6-DCPIP loaded biosorbents; $G = 0 - 100 \mu\text{m}$; $t = 40 \text{ min}$; $v = 150 \text{ rpm}$; $V = 10 \text{ mL}$; at room temperature.

2,6-DCPIP from aqueous solution has been proven. Both materials are efficient biosorbents, but the treated PTT showed better performance than natural PTT. The adsorption was highly dependent on various operating parameters such as; treatment of biosorbent, contact time, pH of solution, biosorbents dosage, initial concentration of 2,6-DCPIP, ionic strength and interfering ions. The adsorption isotherms indicate that the equilibrium data are the best described by the Dubinin-Radushkevich and Temkin isotherms for natural and treated PTT, respectively. Results of adsorption kinetics demonstrated that the adsorption processes were controlled by pseudo-second order kinetics. The mechanism of diffusion was studied and the results showed that external mass transfer was the main rate controlling step. Desorption using NaOH as desorbing agent recovers a maximum quantity of 2,6-DCPIP. From the results obtained, the utilization of PTT for the removal of 2,6-DCPIP from aqueous solution is promising.

Acknowledgements

The authors acknowledge the support of the International Foundation for Science (Grant n° W/5859-1 awarded to Evangeline NJANJA). Financial support from The World Academy of Sciences for the Advancement of Science in Developing Countries (TWAS grant no. 12-117 RG/CHE/AF/AC-G) is gratefully acknowledged.

Conflicts of Interest

The authors declare no conflicts of interest regarding the publication of this paper.

References

- [1] Gupta, V.K. and Suhas (2009) Application of Low-Cost Adsorbents for Dye Removal—A Review. *Journal of Environmental Management*, **90**, 2313-2342. <https://doi.org/10.1016/j.jenvman.2008.11.017>
- [2] Yagub, M.T., Sen, T.K., Afroze, S. and Ang, H.M. (2014) Dye and Its Removal from

- Aqueous Solution by Adsorption: A Review. *Advances in Colloid and Interface Science*, **209**, 172-184. <https://doi.org/10.1016/j.cis.2014.04.002>
- [3] Jalil, A.A., Triwahyono, S., Adam, S.H., Rahim, N.D., Aziz, M.A.A., Haironm, N.H.H., Razali, N.A.M., Abidin, M.A.Z. and Mohamadiah, M.K.A. (2010) Adsorption of Methyl Orange from Aqueous Solution onto Calcined Lapindo Volcanic Mud. *Journal of Hazardous Materials*, **181**, 755-762. <https://doi.org/10.1016/j.jhazmat.2010.05.078>
- [4] Hamad, H.A., Sadik, W.A., Abd El-latif, M.M., Kashyout, A.B. and Feteha, M.Y. (2016) Photocatalytic Parameters and Kinetic Study for Degradation of Dichlorophenol-Indophenol (DCPIP) Dye Using Highly Active Mesoporous TiO₂ Nanoparticles. *Journal of Environmental Sciences*, **43**, 26-39. <https://doi.org/10.1016/j.jes.2015.05.033>
- [5] Mane, V.S. and Babu, P.V.V. (2013) Kinetic and Equilibrium Studies on the Removal of Congo Red from Aqueous Solution Using Eucalyptus Wood (*Eucalyptus globulus*) Sawdust. *Journal of the Taiwan Institute of Chemical Engineers*, **44**, 81-88. <https://doi.org/10.1016/j.jtice.2012.09.013>
- [6] Greluk, M. and Hubicki, Z. (2011) Comparison of the Gel Anion Exchangers for Removal of Acid Orange 7 from Aqueous Solution. *Chemical Engineering Journal*, **170**, 184-193. <https://doi.org/10.1016/j.cej.2011.03.052>
- [7] Ellass, K., Laachach, A., Alaoui, A. and Azzi, M. (2011) Removal of Methyl Violet from Aqueous Solution Using a Stevensite-Rich Clay from Morocco. *Applied Clay Science*, **54**, 90-96. <https://doi.org/10.1016/j.clay.2011.07.019>
- [8] Aki, M.A., Youssef, A.M. and Al-Awadhi, M.M. (2013) Adsorption of Acid Dyes onto Bentonite and Surfactant-Modified Bentonite. *Journal of Analytical and Bioanalytical Techniques*, **4**, 1-7.
- [9] Shanker, M. and Chinnigounder, T. (2012) Adsorption of Reactive Dye Using Low Cost Adsorbent: Cocoa (*Theobroma cacao*) Shell. *World Journal of Applied Environmental Chemistry*, **1**, 22-29.
- [10] Chakraborty, S., Chowdhury, S. and Saha, P.D. (2011) Adsorption of Crystal Violet from Aqueous Solution onto NaOH-Modified Rice Husk. *Carbohydrate Polymers*, **86**, 1533-1541. <https://doi.org/10.1016/j.carbpol.2011.06.058>
- [11] Wan Ngah, W.S. and Hanafiah, M.A.K.M. (2008) Removal of Heavy Metal Ions from Wastewater by Chemically Modified Plant Wastes as Adsorbents: A Review. *Bioresour. Technology*, **99**, 3935-3948. <https://doi.org/10.1016/j.biortech.2007.06.011>
- [12] Benaïssa, H. and Elouchdi, M.A. (2011) Biosorption of Copper(II) Ions from Synthetic Aqueous Solutions by Drying Bed Activated Sludge. *Journal of Hazardous Materials*, **194**, 69-78. <https://doi.org/10.1016/j.jhazmat.2011.07.063>
- [13] Carletto, R.A., Fabiana, C., Francesca, B. and Franco, F. (2008) Adsorption of Congo Red Dye on Hazelnut Shells and Degradation with Phanerochaete Chrysosporium. *Bioresources*, **3**, 1146-1155.
- [14] Albadarin, A.B. and Mangwandi, C. (2015) Mechanisms of Alizarin Red S and Methylene Blue Biosorption onto Olive Stone By-Product: Isotherm Study in Single and Binary Systems. *Journal of Environmental Management*, **164**, 86-93. <https://doi.org/10.1016/j.jenvman.2015.08.040>
- [15] Said, A.E.A., Alyl, A.A.M., El-Wahab, M.M.A., Soliman, S.A.E., El-Hafez, A.A.A., Helmey, V. and Goda, M.N. (2013) An Efficient Biosorption of Direct Dyes from Industrial Wastewaters Using Pretreated Sugarcane Bagasse. *Energy and Environmental Engineering*, **1**, 10-16.

- [16] Ofomaja, A.E. and Ho, Y.-S. (2008) Effect of Temperatures and pH on Methyl Violet Biosorption by *Mansonia* Wood Sawdust. *Bioresource Technology*, **99**, 5411-5417. <https://doi.org/10.1016/j.biortech.2007.11.018>
- [17] Nanseu-Njiki, C.P., Kenne, D.G. and Ngameni, E. (2010) Study of Removal of Paraquat from Aqueous Solution by Biosorption onto Ayous (*Triplochiton Schleroxylon*) Sawdust. *Journal of Hazardous Materials*, **179**, 63-71. <https://doi.org/10.1016/j.jhazmat.2010.02.058>
- [18] Chen, Z., Deng, H., Chen, C., Yang, Y. and Xu, H. (2014) Biosorption of Malachite Green from Aqueous Solutions by *Pleurotus ostreatus* Using Taguchi Method. *Journal of Environmental Health Science and Engineering*, **12**, 1-10. <https://doi.org/10.1186/2052-336X-12-63>
- [19] Chowdhury, S. and Saha, P. (2010) Sea Shell Powder as a New Adsorbent to Remove Basic Green 4 (Malachite Green) from Aqueous Solutions: Equilibrium, Kinetic and Thermodynamic Studies. *Chemical Engineering Journal*, **164**, 168-177. <https://doi.org/10.1016/j.cej.2010.08.050>
- [20] Maznah, W.O.W., Al-Fawwaz, A.T. and Surif, M. (2012) Biosorption of Copper and Zinc by Immobilised and Free Algal Biomass, and the Effects of Metal Biosorption on the Growth and Cellular Structure of *Chlorella* sp. and *Chlamydomonas* sp. Isolated from Rivers in Penang, Malaysia. *Journal of Environmental Sciences*, **24**, 1386-1393. [https://doi.org/10.1016/S1001-0742\(11\)60931-5](https://doi.org/10.1016/S1001-0742(11)60931-5)
- [21] Yargiç, A.S., Sahim, R.Z.Y., Ozbay, N. and Onal, E. (2015) Assessment of Toxic Copper(II) Biosorption from Aqueous Solution by Chemically-Treated Tomato Waste. *Journal of Cleaner Production*, **88**, 152-159. <https://doi.org/10.1016/j.jclepro.2014.05.087>
- [22] Yazici, H., Kiliç, M. and Solak, M. (2008) Biosorption of Copper(II) by *Marrubium Globosum* Subsp. *Globosum* Leaves Powder: Effect of Chemical Pretreatment. *Journal of Hazardous Materials*, **151**, 669-675. <https://doi.org/10.1016/j.jhazmat.2007.06.042>
- [23] Gautam, R.K., Mudhoo, A. and Chattopadhyaya, M.C. (2013) Kinetic, Equilibrium, Thermodynamic Studies and Spectroscopic Analysis of Alizarin Red S Removal by Mustard Husk. *Journal of Environmental Chemical Engineering*, **1**, 1283-1291. <https://doi.org/10.1016/j.jece.2013.09.021>
- [24] Kariuki, Z., Kiptoo, J. and Onyancha, D. (2017) Biosorption Studies of Lead and Copper Using Rogers Mushroom Biomass “*Lepiota Hystrix*”. *South African Journal of Chemical Engineering*, **23**, 62-70. <https://doi.org/10.1016/j.sajce.2017.02.001>
- [25] Panda, H., Tiadi, N., Mohanty, M. and Mohanty, C.R. (2017) Studies on Adsorption Behavior of an Industrial Waste for Removal of Chromium from Aqueous Solution. *South African Journal of Chemical Engineering*, **23**, 132-138. <https://doi.org/10.1016/j.sajce.2017.05.002>
- [26] Chen, A.-H. and Chen, S.-M. (2009) Biosorption of Azo Dyes from Aqueous Solution by Glutaraldehyde-Crosslinked Chitosans. *Journal of Hazardous Materials*, **172**, 1111-1121. <https://doi.org/10.1016/j.jhazmat.2009.07.104>
- [27] Al-Degs, Y.S., El-Barghouthi, M.I., El-Sheikh, A.H. and Walker, G.M. (2008) Effect of Solution pH, Ionic Strength, and Temperature on Adsorption Behavior of Reactive Dyes on Activated Carbon. *Dyes and Pigments*, **77**, 16-23. <https://doi.org/10.1016/j.dyepig.2007.03.001>
- [28] Sangeetha, S., Piyush, C. and Juhee, S. (2014) Investigation on Biosorption of Acidic Dye from an Aqueous Solution by Marine Bacteria, *Planococcus* sp. VITP21. *International Journal of ChemTech Research*, **6**, 4755-4763.

- [29] Wu, Z., Zhong, H., Yuan, X., Wang, H., Wang, L., Chen, X., Zeng, G. and Wu, Y. (2014) Adsorptive Removal of Methylene Blue by Rhamnolipid-Functionalized Graphene Oxide from Wastewater. *Water Research*, **67**, 330-344. <https://doi.org/10.1016/j.watres.2014.09.026>
- [30] Ho, Y.-S., Chiang, T.-H. and Hsueh, Y.-M. (2005) Removal of Basic Dye from Aqueous Solution Using Tree Fern as a Biosorbent. *Process Biochemistry*, **40**, 119-124. <https://doi.org/10.1016/j.procbio.2003.11.035>
- [31] Moussa, A. and Mohamed, T. (2015) Kinetic, Equilibrium and Thermodynamic Study on the Removal of Congo Red from Aqueous Solutions by Adsorption onto Apricot Stone. *Process Safety and Environmental Protection*, **98**, 424-436. <https://doi.org/10.1016/j.psep.2015.09.015>
- [32] Djemmo, L.G., Njanja, T.E., Deussi, M.C.N. and Tonle, K.I. (2016) Assessment of Copper(II) Biosorption from Aqueous Solution by Agricultural and Industrial Residues. *Comptes Rendus Chimie*, **19**, 841-849. <https://doi.org/10.1016/j.crci.2016.01.017>
- [33] Meroufel, B., Benali, O., Benyahia, M., Benmoussa, Y. and Zenasni, M.A. (2013) Adsorptive Removal of Anionic Dye from Aqueous Solutions by Algerian Kaolin: Characteristics, Isotherm, Kinetic and Thermodynamic Studies. *Journal of Materials and Environmental Science*, **4**, 482-491.
- [34] Gusmão, K.A.G., Gurgel, L.V.A., Melo, T.M.S. and Gil, L.F. (2012) Application of Succinylated Sugarcane Bagasse as Adsorbent to Remove Methylene Blue and Gentian Violet from Aqueous Solutions: Kinetic and Equilibrium Studies. *Dyes and Pigments*, **92**, 967-974. <https://doi.org/10.1016/j.dyepig.2011.09.005>
- [35] Sharma, N. and Nandi, B.K. (2013) Utilization of Sugarcane Bagasse, an Agricultural Waste to Remove Malachite Green Dye from Aqueous Solutions. *Journal of Materials and Environmental Science*, **4**, 1052-1065.
- [36] Bharathi, K.S. and Ramesh, S.T. (2013) Removal of Dyes Using Agricultural Waste as Low-Cost Adsorbents: A Review. *Applied Water Science*, **3**, 773-790. <https://doi.org/10.1007/s13201-013-0117-y>
- [37] Fungaro, D.A., Yamaura, M. and Carvalho, T.E.M. (2011) Adsorption of Anionic Dyes from Aqueous Solution on Zeolite from Fly Ash-Iron Oxide Magnetic Nanocomposite. *Journal of Atomic and Molecular Sciences*, **2**, 305-316. <https://doi.org/10.4208/jams.032211.041211a>